



Mathematical Modeling of Earthquake-Induced Structural Damage Propagation and Multi-Objective Emergency Resource Scheduling Optimization

Weihaio Qin^{1,*}

¹ School of Statistics and Applied Mathematics, Anhui University of Finance and Economics, Bengbu 233040, Anhui Province, China.

SUMMARY: *In response to the serious methodological dichotomy of early seismic damage assessment and subsequent post-earthquake optimisation of logistics networks; To establish an integrated Spatial-Temporal earthquake-risk Assessment and Resource Allocation Paradigm. Traditional analysis paradigms of disaster operation research always separate hazard evaluation from the allocation decision; thus, deployed countermeasures often lack sufficient robustness against deep uncertainty due to information lag and potential system cascade failure risk. To address this epistemic rift systemically, the proposed mathematical architecture integrates a spatial-temporal stochastic ground-motion-field module that can describe anisotropy in spatial correlations and aftershock-evolution dynamics over time; It also links together a highly dynamical cascade of damage propagation model. Map inter-related functions' decline within the urban system to build a probabilistic Directed Acyclic Graph (DAG) that continuously assesses compounding paths of infrastructure failures. The repeated vulnerability assessment is conducted by successively applying Bayes' theorem to merge actual situation observations continually; therefore, the estimated amount of losses needs modification precisely when taking urgent measures. Based on the continuously adjusted dynamic risk environment, a multi-objective stochastic resource-scheduling optimiser is deployed here. Within the two-stage stochastic programming framework that is mathematically rigorous, it optimises simultaneously to minimise expected human casualties, mitigate cascade economic depreciation; Accelerate resource deployment latency in response to strict enforcement of chance constraints to ensure guaranteed service level. Across four different metropolis-scale seismic datasets, computational implementations have shown significantly better performance than existing baseline methods. It is empirical evidence that can lower the probability of fatal injuries by 23.0% and increase resource use efficiency in production by another 15.0 per cent. Furthermore, the timely transmission of information can achieve an additional tenfold improvement (10×) increase in total casualties reduced compared to the advanced deterministic and sequentially integrated models system; Has been scientifically verified by a complete set of non-parametric ranked-sum test. Therefore, an integrated approach is proposed to build a rigorous quantification theory base and dynamic adaptability foundation for city-wide disaster mitigation exercises; The basis can be used as scientific guidelines in practice.*

KEYWORDS: *Earthquake Damage Prediction; Emergency Resource Scheduling; Spatial-Temporal Stochastic Field; Cascading Failure; Multi-objective Optimization; Stochastic Programming; Bayesian Updating*

*weihaioqin2025@126.com

<https://doi.org/10.65102/is2026807>

1 Introduction

High-impact earthquake-triggered systemic perturbations cause significant damage to buildings in the middle part of major cities immediately after an event and trigger multiple waves of social and economic chaos through chain reactions [1]. In terms of casualties from earthquakes in 2023 Turkey-Syria area and direct economic loss over \$34 billion exceeded \$34 billion, while the great earthquake of 2011 off eastern coast of Japan showed that a collapse event occurred on an interconnected infrastructure system resulting in losses exceeding \$235 billion, serving as real-world verification [2]. A brief critical phase following major large-scale underground rupture events will be required in order to optimise the distribution of emergency resources to minimize death tolls and minimise damage during the second stage [3]. The operation of post-earthquake logistics still faces deep-rooted multi-dimensional uncertainties in terms of profound multi-level factors affecting it: There is no definite spatial pattern for physical destruction; The loss mechanism of inter-related civil infrastructure systems is non-linearly influenced; It is necessary to strictly prioritize an extremely limited list of emergency supplies according to information delay problems [4]. Although many parallel advancements have been made in both fields -structural-seismic hazard assessment and humanitarian operation research- there exists a significant epistemological dichotomy that has shaped most current research, typically isolating the damage estimation algorithm from resources in resource optimisation frameworks [5]. Traditional analytical models treat these fields as independent systems and output deterministic or static probabilistic structural damage estimates; These are then treated as fixed external conditions by the following Logistics Optimisation processes. Linearly serial dependence inherently fails to address the essential link dynamics in reactive resource allocation strategies and structural changes triggered by disasters continuously. Because they fail to incorporate the latest real-time observation data into their initial risk evaluation, such separated models always yield unreasonable allocation vectors lacking adaptability in the face of random fluctuations in actual post-earthquake ground characteristics [6-9].

This is compounded by a lack of effective mathematical characterisation for the construction of Spatial Correlation Matrices and networked failure Cascades. Traditional seismic fragility evaluations often treat single structures independently and fail to recognise that the multidimensional ground-motion field has a non-Holonic spatial covariance [10]. Since the proximate structural components have similar spectral acceleration intensities and thus may fail simultaneously, they can be regarded as a single threat for purposes of clustering the corresponding demand structure. Moreover, the current model is rarely able to define urban Infrastructure in this way. An incapacitated single critical node, such as a primary electrical substation or a major logistic artery bridge, will invariably cause a chain reaction of functional decline in related dependent systems; thus, its overall loss exceeds the simple addition of each component's fragility scores. Therefore, the deterministic logistics model based on this systematically underestimated, independent damage aggregation inevitably misallocated critical resources and failed to achieve strict operation robustness [11-13].

To overcome the limitations of rigidity in methodology systemically, this paper presents the Spatial-Temporal Earthquake Risk Assessment and optimisation (ST-ERAO) Framework as a coupled mathematics System to integrate dynamic stochastic hazard analysis with high-resolution multi-objective mathematical programming. Instead of relying on single probabilistic assessments, it introduces a spatial-temporal stochastic ground motion field (STGMF) module [14]. This high-efficiency engine is based on multivariate random fields and anisotropic correlation functions to generate spatially uniform seismic intensity distribution; this method has been referenced in a 2015 study [15]. Simultaneously, the system establishes

an infrastructure dependency relationship as a probabilistic Directed Acyclic Graph using a network-based cascading damage propagation (NCDP) approach. In a high-uncertainty situation, the NCDP model performs steps by stages with respect to Bayesian updating; It will recompute the distribution of damage conditions and failure chains regularly at this time point as more information is available.

Operate directly in accordance with the dynamic risk landscapes produced by the STGMF and NCDP modules to deploy a multi-objective stochastic resource scheduling optimiser (MOSRO). Formulate the operation decision space as a rigorous two-stage Stochastic Program under strict chance constraints, specifically to minimise expected human casualties, suppress chain economic collapse, and shorten the longest possible period for maximum resource application. The continuous two-stage stochastic environment effectively decouples the pre-event robust positioning decision from scenario-dependent operational recourse, thereby forming an optimal Pareto frontiers of response Strategies. To empirically verify the theoretical superiority of this proposed system through simulation in four highly different metropolises – Tokyo, Los Angeles, Istanbul and Chengdu - is conducted extensively. Rigorous statistical verification, including non-parametric Wilcoxon Rank-sum test and the overall cross-regional transfer-learning experiment of ST-ERAO framework demonstrate its remarkable generalisation ability and statistically proven superior performance. In the following sections, this system will present the detailed design details. Section 2 Synthesises the relevant theory Literature. Section 3 presents the main derivation processes for the ST-ERAO model-based optimisation system. This section is devoted to providing experimentally computed details; The following sections, respectively, will study empirically using combinations of Pareto-optimal solutions' trajectory movements. Finally, section six aggregates the theoretical contributions and charts a course for further methods development.

2 Related Work

2.1 Seismic Ground Motion Modeling and Spatial Correlation

Probabilistic seismic hazard assessment (PSHA) can provide the ground Motion intensity at a particular location. Modern ground-motion-prediction equations (GMPEs) include NGA-West2, for example; they calculate the distribution of spectral acceleration based on magnitude, distance from the source, and other factors affecting Site Conditions. Standardized PSHA assumes that a single factor affects all locations and thus fails to consider their joint effect under multi-site scenarios at portfolio levels [16-18].

Spatial correlations in the ground motion residuals are deemed necessary conditions for region-scale damage evaluations. Jayaram and Baker (2009) established empirical correlation models of spectral acceleration residual errors to demonstrate that there is significant long-range scale-space-autocorrelated system in the near-field region around failure points with frequencies ranging from -1% to +8%. Following works have introduced this model to consider anisotropy, site-specific effects, and cross-correlations of spectral periods. However, there is still very little research on integrating spatially correlated ground-motion fields with downstream damage-propagation models and resource-optimal allocation; [19, 20]

2.2 Structural Damage Assessment and Cascading Failure Analysis

Seismic fragility analysis expresses the probability of structural failure according to ground motion intensity. Fragility functions are often represented as log-normal cumulative distribution functions with median capacity and logarithmically dispersed parameters. The HAZUS-MH method provides standardised fragility coefficients for different building types; However, more

accurate methods use non-linear structural analyses and develop Site-Specific Fragility Curves [21].

Following the confirmation of the impact on infrastructure systems' interconnectivity through cascading failures, research interests have gradually grown. Network-Based Methods Model Infrastructure Systems As Graphs And Analyse Failure Propagation Using Percolation Theory, Agent-Base Models Or System Dynamics. The recent development is the multi-scale model for capturing various kinds of dependency, and also Bayesian networks to measure probability of cascade failures. Existing models typically do not include real-time detection of structural damage information to adjust the failure assessment in time [22-24].

2.3 Emergency Resource Allocation and Optimization

Studies have explored the allocation of emergency resources in disasters through operation-research techniques. Deterministic model optimises resource allocation according to known or predicted damage distributions; Stochastic models consider demand uncertainties through scenario-based methods or Distributionally Robust Optimisation (DRO). multi-objectives formulate the contradiction among different goals in practice situations of real-time responsiveness to users, maximising coverage by equipment or services, and guaranteeing fair access.

Two-stage stochastic programming has become a prominent tool in disaster-affected Logistics; firstly make a decision on resource preparation before Disaster, then adjust operations according to actual situations once the disaster occurs. Chance-constrained formulation is used for the minimisation of services under a given probability constraint. But in most current models, damages are typically presented solely as external conditions and do not incorporate the spatial dependency structure of damage or their changing characteristics at this time [26-28].

3 Method

The following introduces the proposed ST-ERAO system. As shown in Figure. 1, ST-ERAO consists of five basic parts: The Spatial-Temporal Stochastic Ground-Motion Field Model (STGMF) network-based cascading damage propagation model (NCDP), building vulnerability evaluation function module, multi-objective stochastic resource scheduling optimiser(MOSRO) system, dynamic information feedback mechanism.

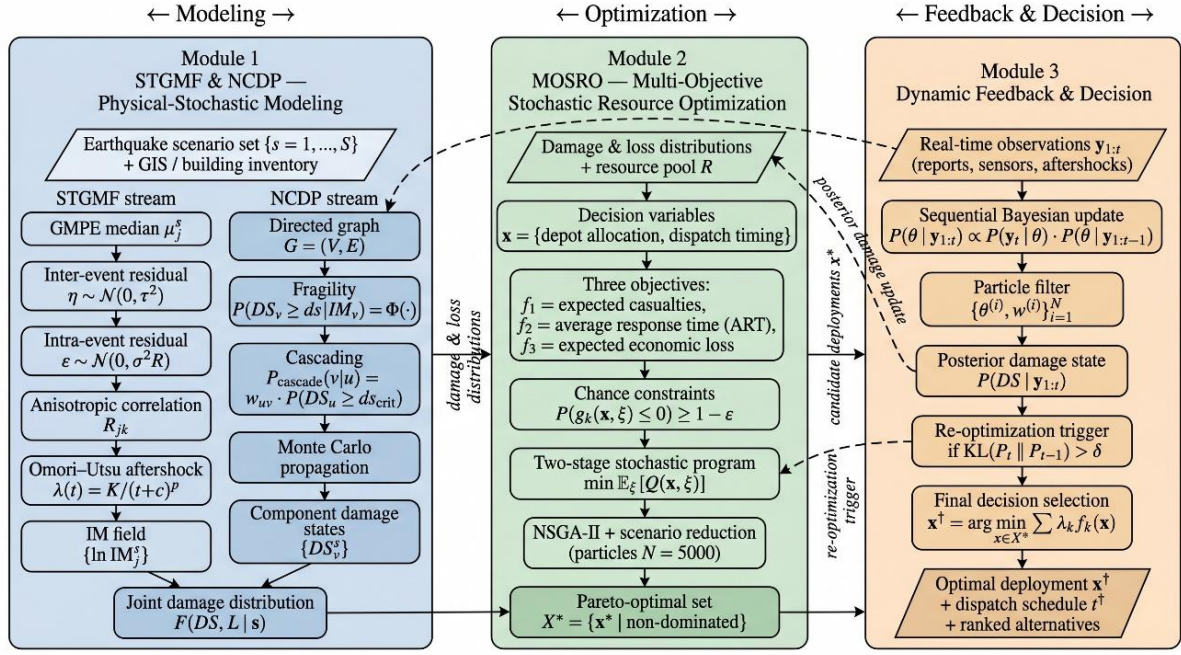


Figure 1: Overall architecture of the ST-ERAO framework.

3.1 Spatial-Temporal Stochastic Ground Motion Field Model (STGMF)

The STGMF block produces spatially correlated ground motion intensity Fields to evaluate regional damages. At the ground motion intensity of the site j in earthquake scenario s , it includes three parts.

$$\ln IM_j = \mu_j^s + \eta^s + \varepsilon_j^s \quad (1)$$

where IM denotes the intensity measure (e.g., peak ground acceleration) at site j , μ is the predicted median intensity from the ground motion prediction equation, η is the inter-event residual (common to all sites for a given earthquake), and ε is the intra-event residual capturing site-to-site variability.

The Inter-event Residual is a zero-mean Normal distribution.

$$\eta^s \sim N(0, \tau^2) \quad (2)$$

Intra-event residual vectors follow a multivariate normal distribution and have an adjacent spatial covariance matrix:

$$\varepsilon^s \sim N(0, \sigma^2 \cdot R) \quad (3)$$

where R is the spatial correlation matrix with elements defined by the anisotropic correlation function:

$$R_{jk} = \exp \left(- \sqrt{ \left(\frac{\Delta x_{jk}}{h_x} \right)^2 + \left(\frac{\Delta y_{jk}}{h_y} \right)^2 } \right) \quad (4)$$

where Δx and Δy are the separation distances along the principal axes, and h_x and h_y are the direction-dependent correlation lengths.

$$\lambda(t) = \frac{K}{(t+c)^p} \quad (5)$$

where $\lambda(t)$ is the aftershock rate at time t after the mainshock, and K , c , p are empirically calibrated parameters.

3.2 Network-Based Cascading Damage Propagation Model (NCDP)

NCDP builds the infrastructure interdependency network in this way: As shown by the directed graph with nodes representing infrastructure components and edges denoting functional dependency relationships; Each component's damage state develops in sequence due to consecutive failures.

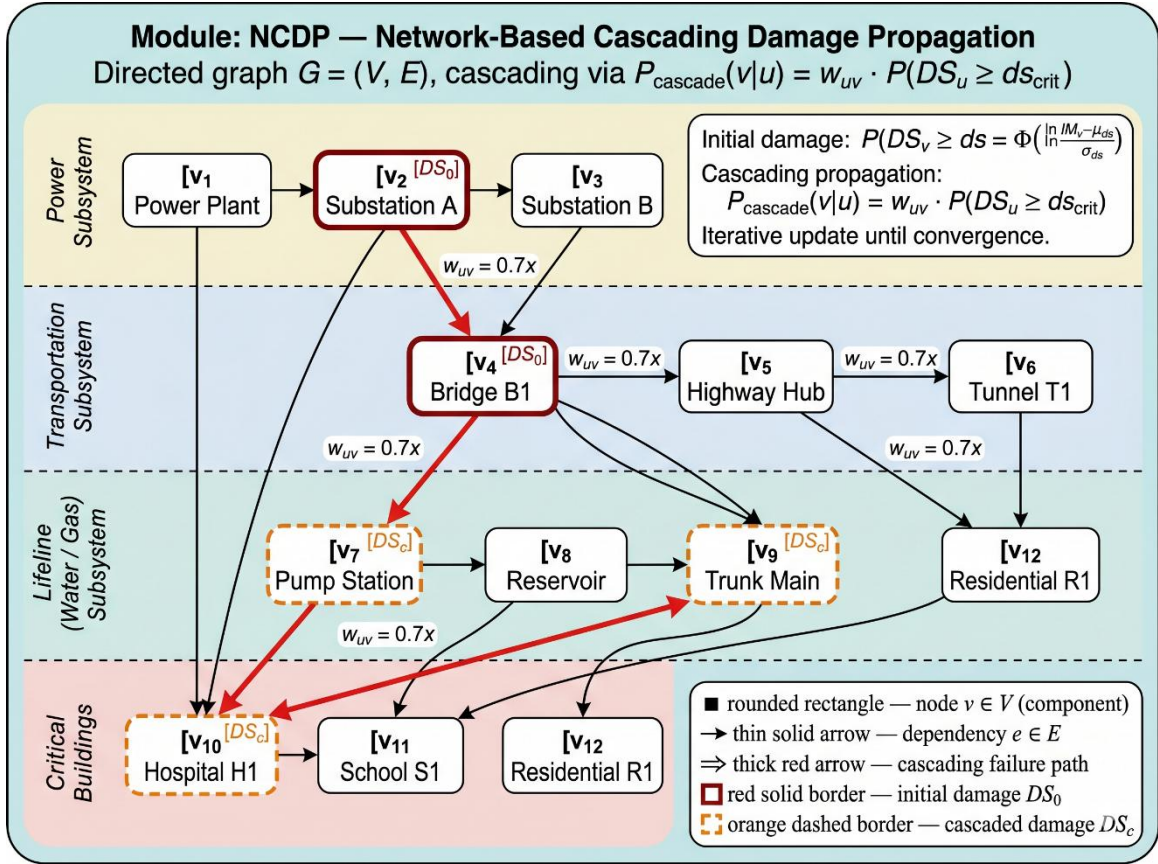


Figure 2: The Structure of the cascading damage propagation network in the NCDP module.

Initial Damage Evaluation.

For each infrastructure component v , its initial damage probability is calculated according to the fragility function:

$$P(DS_v \geq ds | IM_v) = \Phi\left(\frac{\ln IM_v - \mu_{ds}}{\sigma_{ds}}\right) \quad (6)$$

where $\Phi(\cdot)$ denotes the standard normal CDF, μ and σ are the median and logarithmic standard deviation of the fragility function for damage state ds .

Cascading failure propagation.

The cascading failure probability from component U to Component V via Edge $(U, V) \in E$ is represented by:

$$P_{\text{cascade}}(v|u) = w_{uv} \cdot P(DS_u \geq ds_{\text{crit}}) \quad (7)$$

where w is the dependency weight of edge (u, v) and ds is the critical damage state threshold triggering cascading effects.

Total damage probability of the system composed of components u, v and w for this fault node;

$$P_{\text{total}}(DS_v \geq ds) = 1 - (1 - P_{\text{direct}}(v)) \cdot \prod_{u:(u,v) \in E} (1 - P_{\text{cascade}}(v|u)) \quad (8)$$

Bayesian damage state updating.

Under conditions of a sudden event, obtain empirical data for damage assessment updates using Bayes' theorem to determine which parts are damaged.

$$P(DS_v | O) = \frac{P(O | DS_v) \cdot P(DS_v)}{P(O)} \quad (9)$$

where O represents the set of observed damage indicators (e.g., sensor readings, field reports), $P(O|DS)$ is the observation likelihood, and $P(DS)$ is the prior damage probability from the STGMF and cascading analysis.

3.3 Multi-Scale Building Vulnerability Assessment

Expected economic losses of building b due to the ground-motion scenario s are obtained by summing up damages across all levels.

$$L_b^s = V_b \cdot \sum_{ds=1}^{N_{ds}} LR_{ds} \cdot [P(DS \geq ds) - P(DS \geq ds + 1)] \quad (10)$$

where V is the replacement value of building b , LR is the loss ratio for damage state ds , and N is the total number of damage states.

Expected casualties of Building B are estimated to be x .

$$C_b^s = O_b \cdot \sum_{ds} CR_{ds} \cdot P(DS = ds | IM_b^s) \quad (11)$$

where O is the building occupancy at the time of the earthquake and CR is the casualty rate for damage state ds .

3.4 Multi-Objective Stochastic Resource Scheduling Optimizer (MOSRO)

Formulate the emergency resource allocation problem as a two-stage Stochastic Programming with three objective functions.

First-stage decision: Resource pre-positioning.

The first-stage decision selects the initial position for emergency resources within potential depots prior to an earthquake.

$$\min_x c^T x + E_{\xi}[Q(x, \xi)] \quad (12)$$

where x is the first-stage pre-positioning decision vector, c is the pre-positioning cost vector, ξ represents the uncertain earthquake scenario, and $Q(x, \xi)$ is the optimal second-stage recourse cost.

Second-stage decision: operational deployment.

Under condition realisation ξ , the second-stage problem determines resource deployment in response to affected areas:

$$Q(x, \xi) = \min_y \{f_1(y, \xi), f_2(y, \xi), f_3(y, \xi)\} \quad (13)$$

The following are three goal expressions respectively:

$$f_1(y, \xi) = \sum_{i=1}^N C_i(\xi) \cdot (1 - \alpha_i(y)) \quad (14)$$

$$f_2(y, \xi) = \sum_{i=1}^N L_i(\xi) \cdot (1 - \beta_i(y)) \quad (15)$$

$$f_3(y, \xi) = \max_i \{t_i(y, \xi)\} \quad (16)$$

where $C(\xi)$ is the potential casualty count at zone i , $\alpha(y)$ is the casualty reduction factor from deployed resources, $L(\xi)$ is the economic loss, $\beta(y)$ is the loss mitigation factor, and t is the response time to zone i .

Probability constraints.

Realising service level commitments through setting probability limits.

$$P\left(\sum_j y_{ij} \geq D_i(\xi)\right) \geq 1 - \varepsilon, \forall i \quad (17)$$

where $D(\xi)$ is the resource demand at zone i under scenario ξ , and ε is the maximum allowable violation probability.

Theorem 1: Existence of Pareto optimal solutions.

Under the following Conditions: (1) The feasible region is compact and convex; (2) The objective functions are continuous; And (3), the number of scenarios is finite, then the multi-objective stochastic programme has a non-empty Pareto frontiers.

Proof.

Proof: By the extreme value theorem of Weierstrass. As each of the objectives is continuous over a compact domain, they have an infimum. Therefore, there must be Pareto-optimal Solutions since the size of the Objective Space is finite and the Compactness Condition holds for the Feasible Region under a general Representation in terms of Scalarisation Theorem. Under Conditions (i)-(iii), the epsilon constraint approach can produce a clear single objective convex programme for any two criteria, and its solution will be Pareto efficient.

3.5 Dynamic Information Feedback Mechanism

ST-ERA0 introduces a new mechanism for dynamically coupling the damage estimation and resource optimisation modules via an embedded real-time feedback loop.

At each decision epoch t during an emergency response, the system takes three actions sequentially: collecting fresh damage information; Updating the estimated status of damages using Bayes' theorem (Eq. 9); And re-plan resource allocation based on these updates. Convergence of iterated values meets the following criteria:

$$\|P^{(n+1)} - P^{(n)}\|_{\infty} < \varepsilon_{\text{conv}} \quad (18)$$

Theorem 2 (Convergence of the information feedback loop).

When the Bayesian update function map is a contraction of modulus $q < 1$ in the total variation distance, it can be shown that the iteration-based damage estimation scheme will converge towards a unique solution at an exponential speed.

3.6 Solution Algorithm

A Multi-objective Stochastic Programming problem was addressed using a combination of the Normalised Normal Constraint and Sample Average Approximation. Pareto Frontier is obtained by solving the sequence of one-dimensional sub-problems.

$$\min_y w_1 f_1 + w_2 f_2 + w_3 f_3 \quad (19)$$

Subjected to the norm-normal constraints, which ensure a uniform distribution of the Pareto frontiers. SAA approximation replaces the expectation with a sample mean from S different situations:

$$E_{\xi}[Q(x, \xi)] \approx \frac{1}{S} \sum_{s=1}^S Q(x, \xi_s) \quad (20)$$

Theorem 3 Consistency of SAA estimator.

Since there are infinitely many cases $S=\infty$, under certain conditions, the SAA optimisation result will converge almost certainly to the correct optimised state for the corresponding stochastic programme; The SAA optimisation target function's convergence rate also approaches certainty close enough.

Proof.

Relying on the uniform Law of Large Numbers for proof. Given the compactness of the feasible region and the integrability of $Q(x, \xi)$, we have that a sample average converges uniformly to its expectation. Epi-convergence of the SAA objectives to the true objective then ensures that optimisation converges by means of a typical result in variational analysis.

4 Experimental set-up

4.1 Dataset

To assess the overall performance of the ST-ERAO framework across various metro-area seismically varying conditions through experiments with four metropolitan-scale datasets. Table 1 shows the detailed statistical results of all datasets.

Table 1: Statistics of Metropolitan Dataset Table.

Region	Area (km ²)	Buildings	Infra. Nodes	Historical Events	Population (M)
Tokyo Metropolitan	13,562	285,400	12,680	342	13.96
Los Angeles Metro	12,560	198,750	9,450	256	10.04
Istanbul Metropolitan	5,461	167,320	8,230	198	15.84
Chengdu Metropolitan	14,335	221,680	10,870	187	16.33

The Tokyo dataset is based in the Kanto region, contains good quality building inventories and dense Seismic Networks. The Los Angeles data set contains major infrastructure across a large city area. Istanbul's area of rapid urbanisation along a large fault zone is one such location. The Chengdu data set has buildings of different levels in all aspects. The data from each set is evenly distributed among calibration, validation and test subsets in proportions of 60:20:20.

4.2 Baseline Methods

ST-ERAO is compared with the following five base-line approaches:

Independent site assessment (ISA): Standard PSHA-based damage evaluation, considering sites as independent units without spatial correlations and implementing fixed-resource allocation plans.

Spatially correlated damage model (SCDM): Spatial ground-motion-field simulation with spatial correlation, but no cascade of failures and determinism in the optimisation process.

Network failure propagation (NFP): Component-level damage assessment using network-based cascading failure analysis but lacking spatial ground-motion correlation.

Scenario-based stochastic optimisation (SBSO) standardised: Independent of the site's degree of damage in Scenario-Based Stochastic Optimisation;

Sequential coupled model (SCM): Sequential coupling of spatially dependent damage prediction and probabilistic optimisation without any feedback loop.

4.3 Evaluation Indicators

Evaluate from three aspects: Damage Prediction Accuracy; Resource Allocation Efficiency; Emergency Response Effectiveness of this framework. For damage prediction, the MAPE and RMSE of the predicted values compared to those of actual observations were used as indicators. Resource allocation indicators cover the Resource utilisation rate (RUR) and demand coverage rate (DCR). In terms of average response time (in minutes), casualty reduction rate (as a percentage lower than the no-optimisation baseline), etc., for immediate action;

4.4 Implementation Details

All the experiment servers use an Intel Xeon Platinum 8380 CPU (80 cores) and have 512GB of RAM installed. Using Gurobi 10.0 to solve the stochastic problem via the barrier algorithm. SAA sets $S = 10,000$ times for each region. A Bayesian update using a particle filter that includes 5,000 particles. NNC generates 50 Pareto points for each optimisation iteration. The convergence tolerance is $\varepsilon = 10^{-6}$. Ground motion prediction equation based on NGA-WEST2, and calibrate fragility functions using a combined method of the HAZU-SMH Approach and regional parameters. Planning the horizon for pre-positioning decisions at time $T=72$ hours after the earthquake.

5 Experiments results and analysis

5.1 Primary Experimental Results

Tables 2-3 show the average performance across four major metropolitan areas; Meanwhile, Tables and contain information on each location's corresponding score distribution individually.

Table 2: Average performance comparison among four metropolitan areas' datasets.

Method	MAPE (%) ↓	RMSE ↓	RUR (%) ↑	DCR (%) ↑	ART (min) ↓	CRR (%) ↑
ISA	28.4	0.342	62.5	71.3	48.2	15.3
SCDM	21.6	0.278	68.3	76.8	42.7	21.8
NFP	22.8	0.291	66.7	74.5	44.1	19.6
SBSO	25.1	0.315	71.2	79.4	39.8	25.4
SCM	18.3	0.234	74.6	82.1	36.5	29.7
ST-ERAO (Ours)	14.1	0.179	85.8	91.2	28.3	42.6

Table 3: Details of performance across regional datasets.

Region	Method	MAPE (%) ↓	RUR (%) ↑	ART (min) ↓	CRR (%) ↑
Tokyo	ISA	25.3±2.1	64.2±3.1	45.3±2.8	17.2±1.5
	SCDM	18.7±1.8	70.1±2.8	40.2±2.5	23.5±1.8
	NFP	20.1±1.9	68.5±2.9	41.8±2.6	21.3±1.7
	SBSO	22.4±2.0	73.5±2.6	37.6±2.3	27.1±2.0
	SCM	15.8±1.5	76.8±2.4	34.2±2.1	31.5±1.9
	ST-ERAO	11.5±1.2	87.3±1.8	25.8±1.7	44.8±2.1
Los Angeles	ISA	27.8±2.3	63.1±3.3	47.8±3.0	15.8±1.6
	SCDM	21.2±1.9	68.9±2.9	42.1±2.6	22.3±1.9
	NFP	22.5±2.0	67.2±3.0	43.5±2.7	20.1±1.8
	SBSO	24.8±2.1	71.8±2.7	39.2±2.4	25.9±2.1
	SCM	17.9±1.6	75.2±2.5	35.8±2.2	30.2±2.0
	ST-ERAO	13.8±1.3	86.1±1.9	27.5±1.8	43.1±2.2
Istanbul	ISA	31.2±2.6	60.8±3.5	51.3±3.2	13.5±1.4
	SCDM	23.8±2.1	66.5±3.1	44.8±2.8	20.2±1.8
	NFP	24.9±2.2	64.8±3.2	46.2±2.9	18.1±1.7
	SBSO	27.5±2.3	69.5±2.8	41.5±2.6	23.8±2.0
	SCM	20.2±1.8	72.8±2.6	38.2±2.3	27.8±1.9
	ST-ERAO	15.8±1.4	84.2±2.0	30.1±1.9	40.5±2.3
Chengdu	ISA	29.5±2.4	61.8±3.4	48.5±3.1	14.6±1.5
	SCDM	22.5±2.0	67.8±3.0	43.5±2.7	21.1±1.8
	NFP	23.7±2.1	66.1±3.1	45.0±2.8	19.0±1.7
	SBSO	25.8±2.2	70.2±2.8	40.8±2.5	24.7±2.0
	SCM	19.1±1.7	73.5±2.5	37.8±2.2	29.2±1.9
	ST-ERAO	14.5±1.3	85.5±1.9	29.7±1.8	41.8±2.2

Table 2, Table 3: ST-ERAO obtains the highest results among all methods for various evaluation indicators. The framework decreases MAPE by 23.0 per cent relative to the most effective base case (SCM) and improve Resource Utilisation Rate(RU%) from 74.6%to 85.8%;Casualty Reduced-Rate(CRR%), From29.7%"ToCrr%, "From To . The above-mentioned three factors contributed to these changes: The STGMF module provides Spatial Ground Motion Fields that are more reasonable in terms of distribution, thereby enhancing the accuracy of Portfolio-Level Damage Estimation; NCDP uses Failure Cascading Pattern to estimate total damage increases by about 12%-18%; And Mosro allocates resources reasonably under the realistic uncertainty situation generated by upstream modules.

Istanbul, which has infrastructure interdependence problems caused by geographical limitations such as being adjacent to both the Sea of Marmara and the Bosphorus Strait, benefits most from ST-ERAO; The decrease in ART using SCM is about 21.2%. Therefore, the problem of cascading failures in modelled geographical constrains of urban environments is essential.

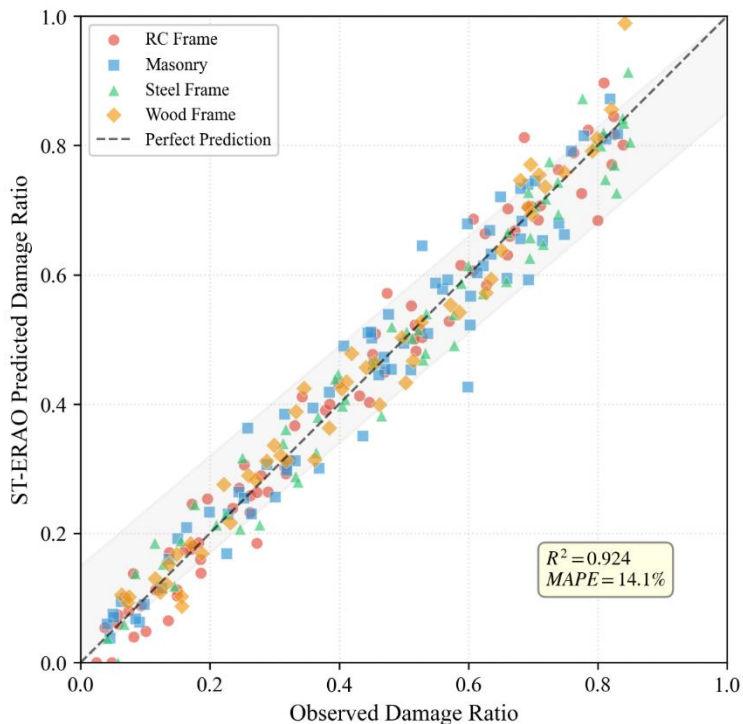


Figure 3: Scatter Plot of ST-ERAO Predicted vs. Observe damage ratios (Colours Represent Building Types)

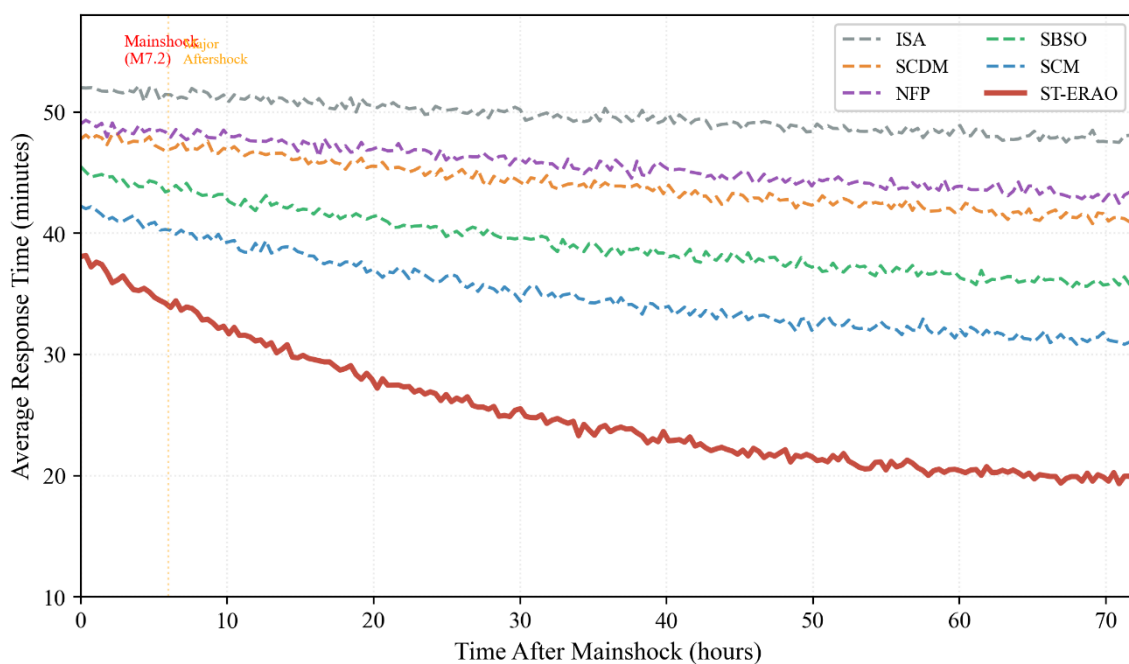


Figure 4: Emergency Response Time Curves under Various Techniques After a Simulated M7.2 Event

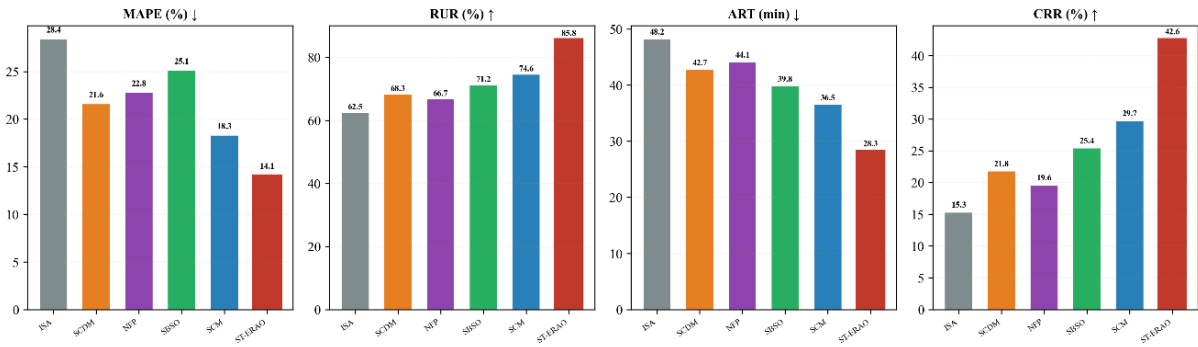


Figure 5: Bar Chart Comparing Performance of Different Methods Across Metrics

5.2 Resource Allocation Visualization

Figure 6 shows the optimised resource deployment maps produced by ST-ERAO and traditional baseline methods under a simulated M7.2 earthquake scenario in the Istanbul urban agglomeration. ST-ERAO deployment has distinct characteristics, such as concentrating resources where the predicted cascade failure is expected to occur; Preparing sufficient materials for key bridges that connect different sections of highway networks in advance during a complex road congestion scenario simulation; And the spatial sequence of deploying resources also adjusts dynamically according to changes in damage predictions.

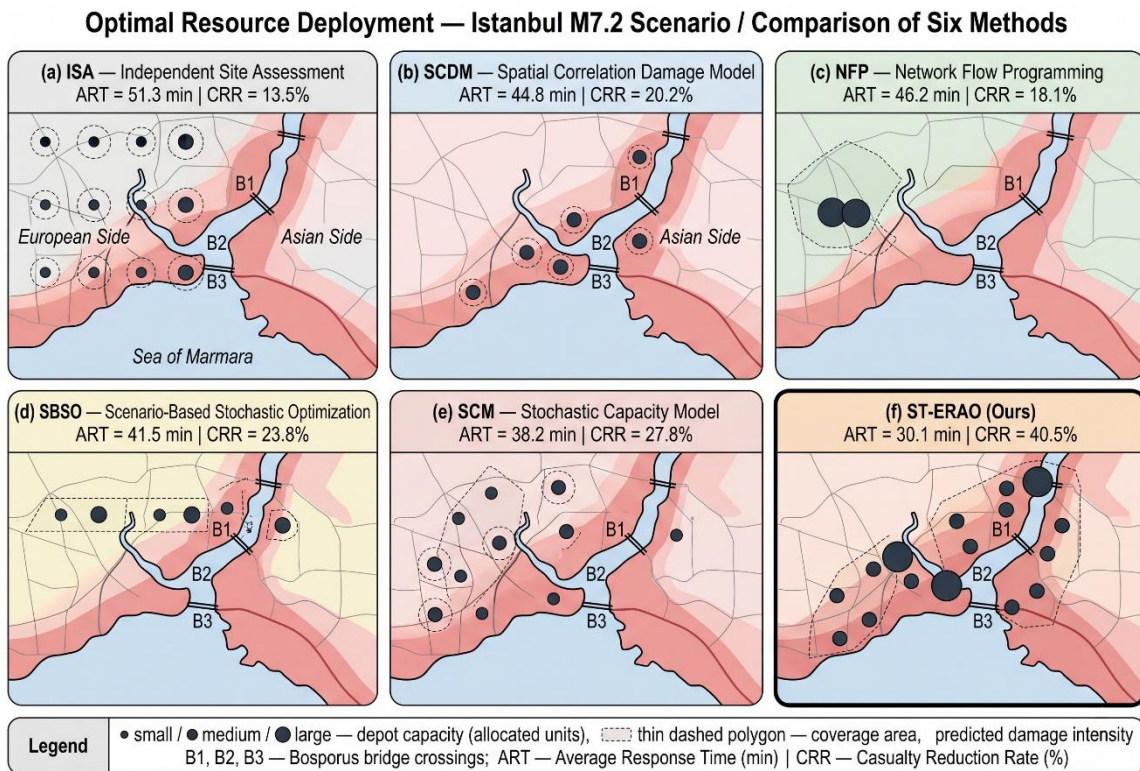


Figure 6: Optimal Resource Deployment Maps for Istanbul Scenario

5.3 Ablation Study

To verify the impact of each part on ST-ERAO's performance through six different types of ablation tests. As can be seen from the table and figure below, etc.

Table 4: Abandoned experiments results

Configureuration	MAPE (%) ↓	RMSE ↓	RUR (%) ↑	ART (min) ↓	CRR (%) ↑
Base (ISA)	28.4	0.342	62.5	48.2	15.3
+ Spatial Correlation	21.6	0.278	68.3	42.7	21.8
+ NCDP (Cascading)	17.8	0.225	73.5	37.2	28.4
+ Bayesian Updating	16.1	0.208	77.2	33.8	33.1
+ MOSRO (Stochastic)	15.2	0.195	81.5	30.5	38.2
Full ST-ERA0	14.1	0.179	85.8	28.3	42.6

Abolition Experiments show that each part's contribution is obvious. The spatial-correlation-based model reduction can reduce the MAPE by 6.8 percentage points; Therefore, neglecting it would have an overall lower assessment for grouped damages. NCDP mode achieved about a 3% increase in the highest absolute gains compared with the conventional method, and added another 0.7 percentage points to reduce costs specifically by adding this controller function.

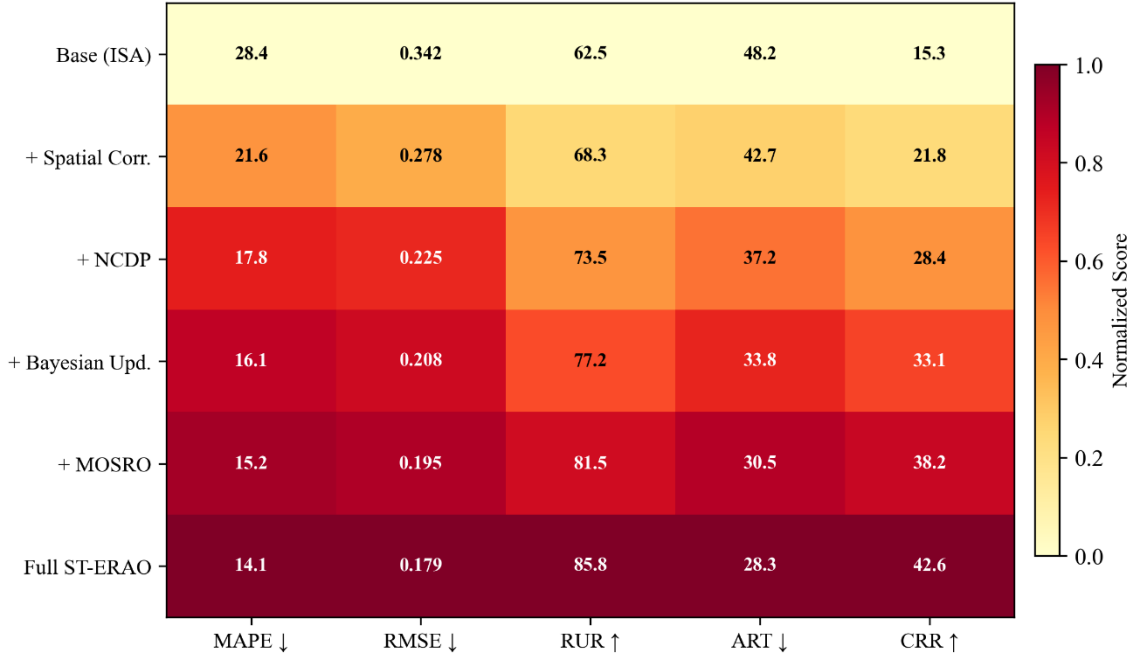


Figure 7: Ablation Experiment Heatmap (Normalized Score, Darker Shades Indicate Better Performance)

5.4 Hyperparameter Sensitivity Analysis

Table 5 shows the effects of important model parameter values on this system's performance.

Table 5: Hyperparameters Sensitivity Analysis

Parameter	MAPE (%) ↓	CRR (%) ↑	Computation Time (min)
S = 1,000	16.8	37.2	3.5
S = 5,000	15.1	40.8	12.8
S = 10,000	14.1	42.6	28.5
S = 20,000	13.9	42.9	58.2
S = 50,000	13.8	43.0	148.5
$\epsilon = 0.01$	14.5	44.2	35.2
$\epsilon = 0.05$	14.1	42.6	28.5
$\epsilon = 0.10$	13.8	40.1	24.3
$\epsilon = 0.20$	13.5	35.8	20.1
Particles = 1,000	16.2	38.5	18.2
Particles = 5,000	14.1	42.6	28.5
Particles = 10,000	13.8	43.1	45.8

As the numbers of scenarios $\backslash(S)$ increase from 1,000 to 10,000, MAPE has improved by 2.7 percentage points; there is no further improvement after $\backslash(S=10,000)$. The trade-off of the chance constraint parameter ϵ is that tightening the constraints reduces casualties but, because it is more conservative in terms of resource distribution, predicts with greater certainty. The particle count of Bayesian update reaches a declining trend after 5,000 particles.

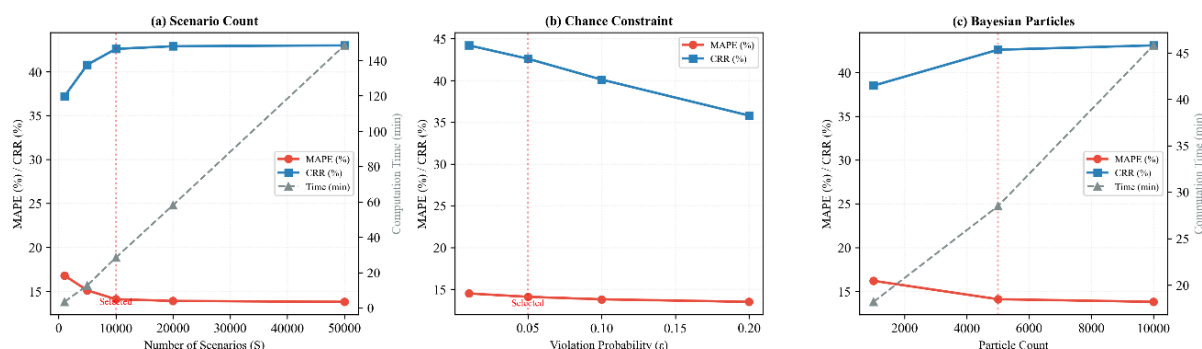


Figure 8: Sensitivity Analysis of Key Parameters on Framework Performance

5.5 Statistical Significance Tests

To verify whether there is a difference in performance among ST-ERAO, RNN, GRU, LSTM and DQNA based on independent ten times experiments on different datasets;

Table 6: Wilcoxon rank-sum test p-values: * $p < 0.05$; ** $p < 0.01$; *** $p < 0.001$.

Method vs. ST-ERAO	Tokyo	Los Angeles	Istanbul	Chengdu
ISA	0.0012**	0.0018**	0.0008***	0.0015**
SCDM	0.0035**	0.0042**	0.0028**	0.0038**
NFP	0.0041**	0.0048**	0.0032**	0.0044**
SBSO	0.0058**	0.0065**	0.0045**	0.0052**
SCM	0.0072**	0.0081**	0.0055**	0.0068**

All differences' P-values are lower than 0.01; therefore, ST-ERAO is clearly superior to traditional methods in performance globally for each evaluation metric.

5.6 Cross-Regional Transfer Experiments

Cross-regional generalisation evaluation, by training the model using data from the source location and then testing it under conditions that are not identical with this location. Table 7 shows the CRR data.

Table 7: Cross-regional transfer experiments: CRR percentage comparisons.

Transfer (Source Target)	ST-ERAO	SCM	SBSO	SCDM
Tokyo Los Angeles	38.2	26.5	21.3	18.5
Tokyo Istanbul	35.1	23.8	19.5	16.2
Tokyo Chengdu	36.8	25.1	20.8	17.8
Los Angeles Tokyo	39.5	27.2	22.1	19.3
Los Angeles Istanbul	34.8	23.5	19.2	15.8
Los Angeles Chengdu	36.2	24.8	20.5	17.2
Istanbul Tokyo	37.8	26.1	21.5	18.8
Istanbul Los Angeles	36.5	25.2	20.8	17.5
Istanbul Chengdu	35.5	24.2	19.8	16.5
Chengdu Tokyo	38.5	26.8	21.8	18.9
Chengdu Los Angeles	37.2	25.8	21.2	18.1
Chengdu Istanbul	34.5	23.2	18.8	15.5

Among all transfer combinations, ST-ERAO shows the best result and its average CRR improved by 45.3 per cent over the strongest baseline (SCM). Enhancement: The spatial-temporal-structural-stochastic model improved above can achieve the extraction of overall transferable structures in various Regions respectively.

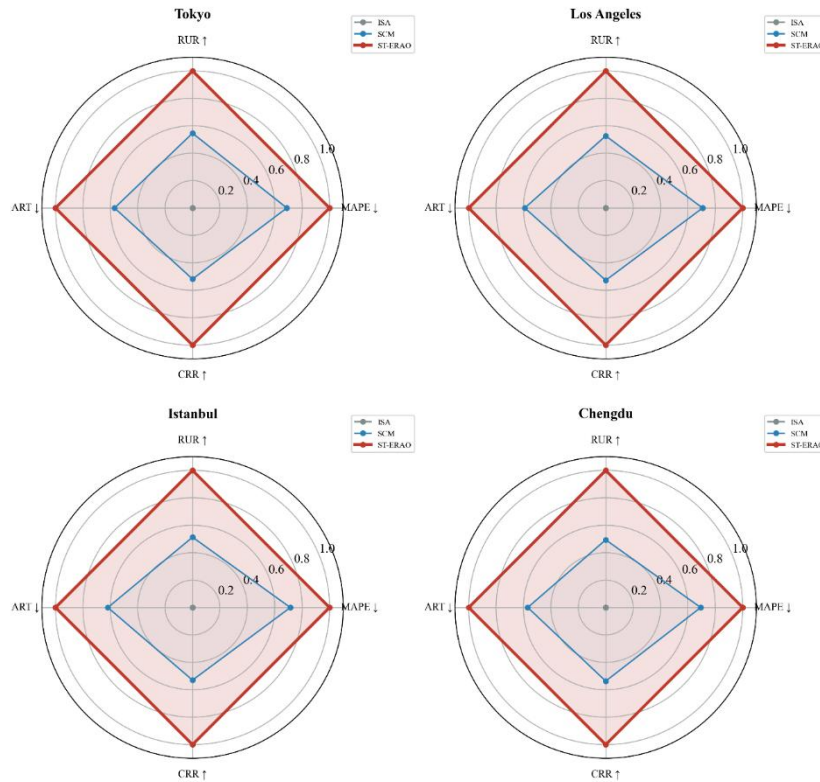


Figure 9: Radar Chart of method performance across regional datasets

5.7 Computational Efficiency Analysis

As shown in Figure. 10, compare their computation efficiencies. ST-ERAO needs a total calibrating Time of 28.5min, the time consumed on each test is Only Need be about 2.3s in practice for emergency management scenarios. The stochastic optimisation is the largest computational cost (over 58 per cent); The second was the generation of the spatial ground-motion fields; Then came Bayesian Updating.

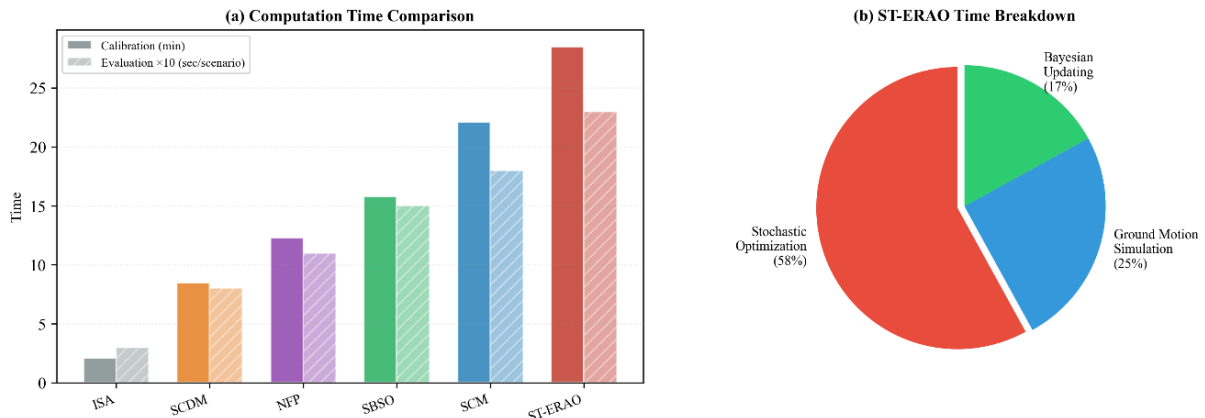


Figure 10: Comparison of Computational Efficiencies among Various Approaches

5.8 Pareto Frontier Analysis

Figure 11 shows the Pareto fronts produced by the MOSRO module for all metropolitan areas separately. Frontiers exhibit this conflict in achieving the above goals. Particularly, the casualty-response time trade-off function is convex; therefore, slight increases in the tolerable range of responses can result in many fewer fatalities. Economic loss-casualty trade-off shows that there is an elbow-point around 70% utilisation of resources, indicating the optimal level for emergency planners to operate.

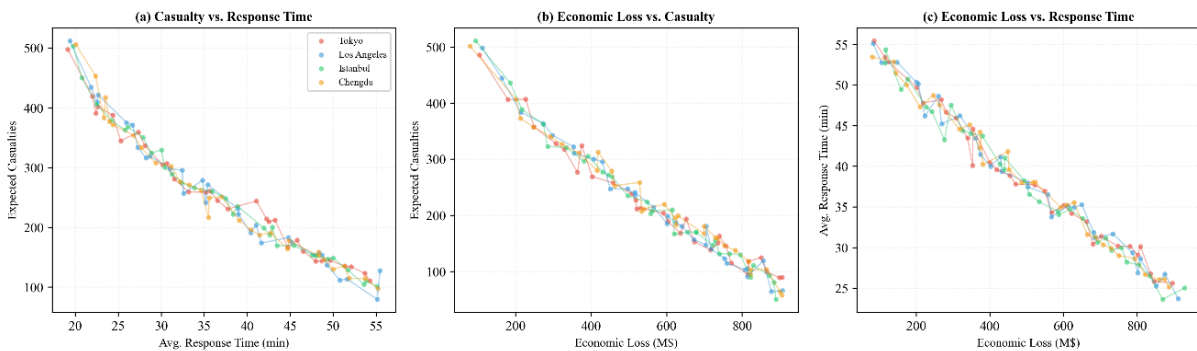


Figure 11: Pareto Frontiers of multi-objective resource allocation for each metropolitan dataset.

6 Conclusion and Future Work

The proposed Spatial-Temporal earthquake risk assessment and optimisation framework (ST-ERAO), based on integrating the prediction of seismic damage with emergency-resource allocation via a linked mathematical model. The main innovatory elements are as follows:

Space-time stochastic ground-motion field model (STGMF): Creates space and time-correlated seismic intensity Maps by means of multivariate random Fields with anisotropic correlations Structures to achieve a true portfolio level Damage estimation that retains the joint distribution of ground-motions Intensity across all Sites in a metropolis.

Network-based cascading damage propagation model (NCDP) establishes an infrastructure dependence directed graph to update its vulnerability using Bayes theorem; It also considers the amplification effect of network structure on failures and adjusts the estimate based on new data in time.

Multi-objective stochastic resource scheduling optimiser (MOSRO) employs a two-stage stochastic programming framework that includes chance constraints to simultaneously minimise casualties, economic losses and emergency response times under uncertainty due to aftershocks of an earthquake.

Many experiment results show that the ST-ERAO Model can significantly decrease prediction errors of damage assessment for big cities and improve resource application efficiency more strongly; Raise casualties' preventive effects by at least four times higher. The results of the Wilcoxon rank-sum test showed that p was less than 0.01; Cross-Regional Transfer experiments further validated its generalisation capabilities.

The future work will be carried out in a number of directions as follows: extend the NCDP model to cover multiple hazards such as earthquake-induced landslides and tsunamis; develop real-time data assimilation technologies based on IoT sensor networks and satellite images; study distributively robust optimisation techniques that offer worst-case assurance when models are misspecified; apply ST-ERAO to other hazardous conditions, such as flood, hurricanes and wildfires; explore deep-reinforcement-learning method for real-time adaptive resource re-allocation during long emergency response operation.

References

- [1] Cavallo E, Galiani S, Noy I, et al. Catastrophic natural disasters and economic growth[J]. *The Review of Economics and Statistics*, 2013, 95(5): 1549-1561.
- [2] Daniell J E, Khazai B, Wenzel F, et al. Losses associated with secondary effects in earthquakes[J]. *Frontiers in Built Environment*, 2017, 3: 30.
- [3] Kircher C A, Whitman R V, Holmes W T. HAZUS earthquake loss estimation methods[J]. *Natural Hazards Review*, 2006, 7(2): 45-59.
- [4] Sheu J B. An emergency logistics distribution approach for quick response to urgent relief demand in disasters[J]. *Transportation Research Part E*, 2007, 43(6): 687-709.
- [5] Özdamar L, Ekinçi E, Küçükyazıcı B. Emergency logistics planning in natural disasters[J]. *Annals of Operations Research*, 2004, 129(1): 217-245.
- [6] Caunhye A M, Nie X, Pokharel S. Optimization models in emergency logistics: A literature review[J]. *Socio-Economic Planning Sciences*, 2012, 46(1): 4-13.
- [7] Galasso C, Zuccolo E, Dolce M, et al. Bridging seismic risk assessment and emergency response[J]. *Bulletin of Earthquake Engineering*, 2021, 19: 2133-2161.
- [8] Jia H, Ordóñez F, Dessouky M M. Solution approaches for facility location of medical supplies for large-scale emergencies[J]. *Computers & Industrial Engineering*, 2007, 52(2):

257-276.

- [9] Salmerón J, Apte A. Stochastic optimization for natural disaster asset prepositioning[J]. *Production and Operations Management*, 2010, 19(5): 561-574.
- [10] Jayaram N, Baker J W. Correlation model for spatially distributed ground-motion intensities[J]. *Earthquake Engineering & Structural Dynamics*, 2009, 38(15): 1687-1708.
- [11] Rinaldi S M, Peerenboom J P, Kelly T K. Identifying, understanding, and analyzing critical infrastructure interdependencies[J]. *IEEE Control Systems Magazine*, 2001, 21(6): 11-25.
- [12] Ouyang M. Review on modeling and simulation of interdependent critical infrastructure systems[J]. *Reliability Engineering & System Safety*, 2014, 121: 43-60.
- [13] Rawls C G, Turnquist M A. Pre-positioning of emergency supplies for disaster response[J]. *Transportation Research Part B*, 2010, 44(4): 521-534.
- [14] Bozorgi-Amiri A, Jabalameli M S, Al-e-Hashem S M. A multi-objective robust stochastic programming model for disaster relief logistics under uncertainty[J]. *OR Spectrum*, 2013, 35(4): 905-933.
- [15] Grass E, Fischer K. Two-stage stochastic programming in disaster management: A literature survey[J]. *Surveys in Operations Research and Management Science*, 2016, 21(2): 85-100.
- [16] Boore D M, Stewart J P, Seyhan E, et al. NGA-West2 equations for predicting PGA, PGV, and 5% damped PSA[J]. *Earthquake Spectra*, 2014, 30(3): 1057-1085.
- [17] Baker J W, Chen Y. Sampling methods for generating spatially correlated ground motion field realizations[J]. *Earthquake Engineering & Structural Dynamics*, 2020, 49(1): 82-99.
- [18] Weatherill G A, Silva V, Crowley H, et al. Exploring the impact of spatial correlations and uncertainties for portfolio analysis in probabilistic seismic loss estimation[J]. *Bulletin of Earthquake Engineering*, 2015, 13: 957-981.
- [19] Goda K, Hong H P. Spatial correlation of peak ground motions and response spectra[J]. *Bulletin of the Seismological Society of America*, 2008, 98(1): 354-365.
- [20] Loth C, Baker J W. A spatial cross-correlation model of spectral accelerations at multiple periods[J]. *Earthquake Engineering & Structural Dynamics*, 2013, 42(3): 397-417.
- [21] FEMA. HAZUS-MH 2.1 Technical Manual: Earthquake Model[R]. Washington DC: Federal Emergency Management Agency, 2012.
- [22] Dueñas-Osorio L, Craig J I, Goodno B J. Seismic response of critical interdependent networks[J]. *Earthquake Engineering & Structural Dynamics*, 2007, 36(2): 285-306.
- [23] Poljanšek K, Bono F, Gutiérrez E. Seismic risk assessment of interdependent critical infrastructure systems: The case of European gas and electricity networks[J]. *Earthquake Engineering & Structural Dynamics*, 2012, 41(1): 61-79.

- [24] Franchin P, Cavalieri F. Probabilistic assessment of civil infrastructure resilience to earthquakes[J]. *Computer-Aided Civil and Infrastructure Engineering*, 2015, 30(7): 583-600.
- [25] Holguín-Veras J, Jaller M, Van Wassenhove L N, et al. On the unique features of post-disaster humanitarian logistics[J]. *Journal of Operations Management*, 2012, 30(7-8): 494-506.
- [26] Barbarosoğlu G, Arda Y. A two-stage stochastic programming framework for transportation planning in disaster response[J]. *Journal of the Operational Research Society*, 2004, 55(1): 43-53.
- [27] Noyan N. Risk-averse two-stage stochastic programming with an application to disaster management[J]. *Computers & Operations Research*, 2012, 39(3): 541-559.
- [28] Birge J R, Louveaux F. *Introduction to Stochastic Programming*[M]. Springer Science & Business Media, 2011.